IOP Conference Series: Earth and Environmental Science

PAPER • **OPEN ACCESS**

Experimental Study on the Unconfined Compressive Strength of Artificially Cemented Sand

To cite this article: Xumin Wang *et al* 2019 *IOP Conf. Ser.: Earth Environ. Sci.* **283** 012002

Experimental Study on the Unconfined Compressive Strength of Artificially Cemented Sand

Xumin Wang, Cheng Wang and Zhao Yi

School of Civil Engineering & Architecture, Hubei University of Technology, Wuhan, Hubei 430068, China.
Email: 425538790@qq.com

Abstract. Artificially cemented sand sample was prepared by incorporating cement clinker into the standard sand sample. The electron microscopic scanning test (SEM) and the unconfined compressive strength test of the artificial cementation sand sample were carried out, and the microstructure changes before and after the cementation of the sand sample were analyzed. The formula of the unconfined compressive strength of cemented sand samples considering the influence of cement clinker incorporation ratio Cv and curing time t is proposed. Scanning electron microscopy experiments show that as the incorporation ratio increases, the standard sand gap is gradually filled by the cements, and the shape of the cements attached to the surface of the standard sand changes from flocculant filamentous to pellet. The unconfined compressive strength test shows that the axial strain decreases with the increase of the blending ratio, and the brittle fracture is more and more obvious. The fitting formula of the unconfined compressive strength is proved to be reasonable by the experimental data of other scholars.
Keywords: Cemented sand; Stress-strain relationship; Incorporation ratio; Maintenance time; Unconfined compressive strength.

1. Introduction

For a long time, scholars have studied the various structures of natural soil and the causes of its formation. The structure of soil refers to the arrangement of soil particles and the cementation between particles. Due to the different sources of inter-particle cementing materials, structural soils are divided into natural structural soils formed under natural conditions and artificially cemented soils formed by adding cement or other chemical cementing materials in undisturbed soils (Li Jianhong 2008). Based on the understanding of the characteristics of soil structure, geotechnical researchers have done a lot of mechanical tests on this. However, in the process of sampling and sample preparation of natural structural soil, it is easy to destroy the cementation property, and it is difficult to obtain a relatively uniform sample (Wei Rulong 1986), thus affecting the study of soil. Due to the great advantage in controlling the structural properties, artificially cemented samples can have similar physical properties to the natural undisturbed soil. Therefore, when studying the mechanical properties of structural soils in the laboratory, artificial methods for preparing structural soil samples are often used. As far as artificially cemented sands are concerned, the existing studies are confined to their immediate interests.

Due to the long period of natural cementation and the preparation and curing of artificially cemented soil for less than one year, the research on artificial sample preparation is in full swing (Zhao Can 2013). In the researchers' various methods for preparing artificially cemented soil (Mitchell

J and Soga K 2005; Saxena S K and Lastrico M 1987; Clough G W et al. 1987; Maccarini M 1987), the method of incorporation of gelling substances is the most widely studied, and the other two methods are CIPS sample preparation method and electrochemical cementation method. Commonly used cementing materials are cement, gypsum, lime, fly ash, etc. The cementing principle is that the chemical reaction between the gel and the soil sample under certain environmental conditions produces a more stable structure than the original soil sample. At present, cemented cement has been widely used in engineering. Zhang Tianhong et al (Zhang Tianhong et al. 2003) studied the effects of cement incorporation ratio, curing age, the addition of improver, wet soaking and initial conditions on strength growth by conducting indoor cement stabilization tests on soft clay. Ruan Jinlou et al. (Ruan Jinlou et al., 2009) combined the experimental results of the mixing ratio of silty clay and cement-soil, to study the relationship between the unconfined compressive strength of cement soil and cement incorporation ratio and age. Therefore, this paper uses cement clinker as a cementitious material and a single standard quartz sand as a soil sample, artificially prepared cement cemented sand sample. Through the unconfined compressive strength test, the variation law of unconfined compressive strength of artificially cemented sand with different cement clinker blending ratio and curing time was studied. At the same time, combined with scanning electron microscopy test, the microscopic morphology of artificially cemented sand before and after cementation features were compared and analyzed.

2. Test Materials and Solutions

2.1. Test Materials

The cementitious material of this test is cement clinker, and the test soil sample is Xiamen ISO standard sand (SiO_2>99%). The particle size range of quartz sand is 0.075mm~2mm, which meets the requirements of mechanical experiments. The quartz sand is dried before use. The particle grading curve is shown in Figure 1. The relative density of soil particles was measured by the pycnometer method, G_s≈2.65, the minimum dry density was 1.54 g/cm^3, the maximum dry density was 1.81 g/cm3, the maximum void ratio was 0.72, and the minimum void ratio was 0.46. The particle size parameters are shown in Table 1. It can be seen from Table 1 that quartz sand is a medium sand with poor gradation.

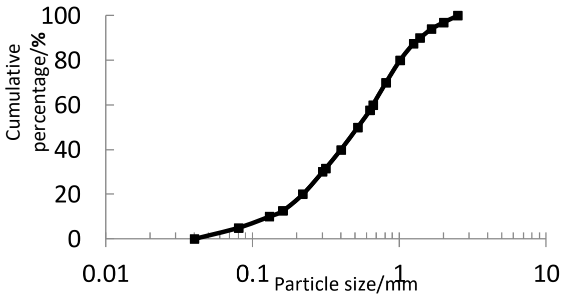

Figure 1. Standard sand sample particle grading curve.

Table 1. Diameter parameters of quartz sand.

d_{95} (*mm*)	d_{60} (*mm*)	d_{50} (*mm*)	d_{30} (*mm*)	d_{10} (*mm*)	C_u	C_c
1.855	0.915	0.763	0.287	0.151	6.060	0.499

The standard sand was subjected to X-ray diffraction analysis by crushing the solidified portion through a 200 mesh sieve. It is found from Figure 2 that the main component of the standard sand is SiO_2, and contains a trace amount of metal elements such as Al, Fe and the like.

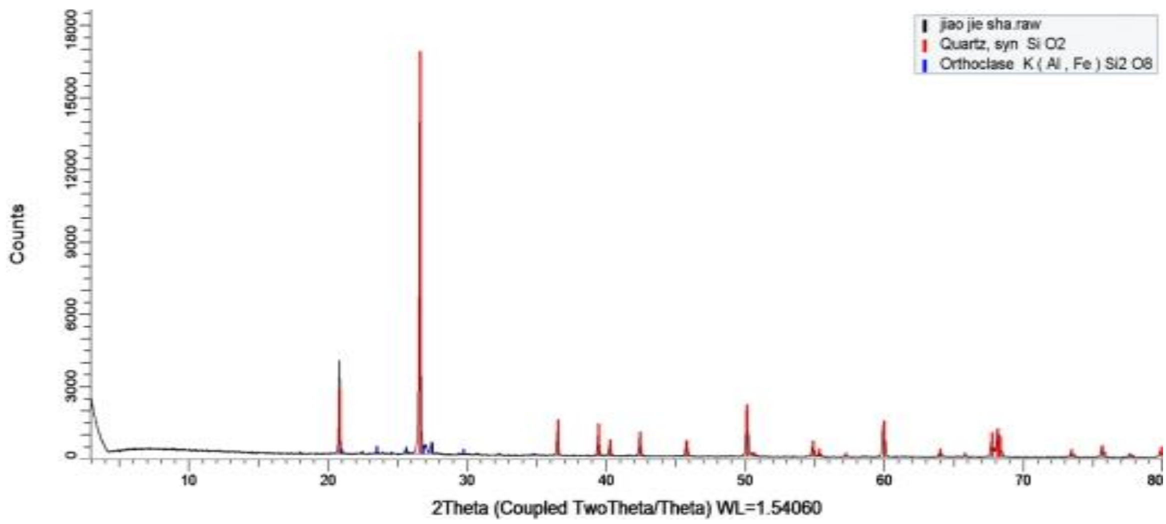

Figure 2. XRD map of the Standard sand.

2.2. Preparation of Samples

According to the "Highway Geotechnical Test Procedures" (JTGE40-2007) disturbing soil sample preparation requirements, the mixed sand will be divided into detachable sample tubes, which will be compacted in 5 layers. The diameter of the sample is 39mm and the height is 80mm, sample preparation parameters are shown in Table 2. The preparation process is as follows: the dried quartz sand is used as the raw material soil, and a certain proportion of clinker (2%, 3%, 5%) is mixed in the raw material soil to form a mixed soil, and the mixed soil is dried at a density of 1.65 g/cm^3. Add water to make the moisture content of the sample reached 10%. After the sample is prepared, it is placed in a constant temperature and humidity chamber at 20 ℃ for curing.

Table 2. Sand samples preparation parameters of unconfined compressive strength tests.

Dry density of sample ρ_d (g/cm^3)	Dry quality of sample (g)	Quartz sand quality (g)	Incorporation ratio C_V (%)	Quality of cement clinker (g)	Moisture content w (%)	Quality of water adulterate (g)
1.65	157.69	154.60 153.10 150.18	2 3 5	3.09 4.59 7.51	10	15.77

2.3. Experimental Design and Method

The unconfined compression test is performed on a triaxial apparatus of strain control that automatically adjusts the strain rate of the test process by removing the pressure chamber. In this paper, the unconfined compressive strength testis carried out for cemented sand samples with a incorporation ratio of 2%, 3%, 5%, and curing time of 1d, 3d, 5d, 7d, 14d, 28d, a total of 18 sets of orthogonal tests, each set of 4 parallel samples. The experimental scheme is shown in Table 3. The axial strain rate of the unconfined compressive strength test should be 1%~3%/min, and the sample is taken as 0.800mm/min. After each set of tests, the mean value of the four intensity values obtained from the test was taken as the unconfined compressive strength value $q_{u.}$ If the intensity value of a group of samples is less than 2 after rejection, the test results of this group are invalid. The experimental scheme is shown in Table 3.

The test procedure is as follows: Before starting the test, the sample that has been cured is measured, the diameter D of the upper, middle and lower parts of the sample were measured respectively, the height H of the sample was measured in three different directions, and the average value of the three data was taken for the diameter D and height H of the sample. The experimental data are collected automatically by computer. The unconfined compressive strength of the sample is taken as the peak strength of the stress curve or the strength corresponding to 15% of the strain.

Table 3. Scheme of unconfined compressive strength tests.

Cement clinker incorporation ratio C_v (%)	Curing time t (d)	Experiment title
2	1,3,5, 7, 14, 28	The unconfined compressive strength test
3	1, 3, 5, 7, 14, 28	
5	1, 3, 5, 7, 14, 28	

3. Analysis of Test Results

According to the experimental design, the experimental study on the unconfined compressive strength of artificially cemented sand under different cement clinker content and curing time conditions were carried out. The results are shown in Table 4.

Table 4. Lab results of unconfined compressive strength tests.

Incorporation ratio/%	Curing time/d					
	1	3	5	7	14	28
2	23.50	52.93	68.83	74.90	93.55	107.75
3	71.98	162.03	200.44	283.84	326.50	387.73
5	102.27	283.05	374.80	438.90	526.53	602.45

3.1. Analysis of Stress and Strain Curve and Failure Characteristics and Cementation Essence

Figure 3 shows the unconfined compressive strength test (USC) stress-strain curve (cultured for 7 days) of samples with different cement clinker contents at a dry density of 1.65 g/cm^3 and a moisture content of 10%. It can be seen from Figure 3 that in the curve of different cement clinker content, the axial stress increases slowly with the increase of strain and then approaches linearity to reach the peak value, and then gradually decreases with the increase of strain until the end of the experiment. The strength of samples with cement clinker incorporation ratio C_v=2% did not decrease rapidly after reaching the limit, but decreased slowly. Therefore, the samples had a certain elasticity. With the increase of incorporation ratio, the failure characteristic is the transition from elastic failure to brittle failure. The higher the content of cement clinker, the more obvious the brittle change.

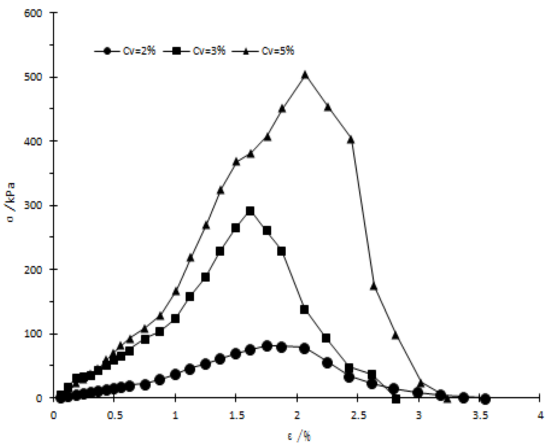

Figure 3. Stress-strain curves of artificially sand in 7 days.

In the microscopic figure of the sample shown in Figure 4, the four groups of sand particles have clear skeleton, most of which are angle-shaped and sub-angle-shaped. The intergranular framework supports each other to form the pores of the scaffold. No cementation crystals were found in the standard sand samples as shown in Figure 4a, with only a few small grains attached to the surface of large particles. In the SEM image of the cemented sand sample, the products such as hydrated calcium silicate and calcium carbonate show obvious, and the size of the crystal particles varies. Most precipitate particles adhere to the surface of the skeleton particles, and some cementites accumulate in the landfill particle gaps due to the continuous hydration reaction of cement clinker. Under the condition of lower incorporation ratio, most of the flocculating cement is attached to the surface of the standard sand, the aggregate of the aggregate is less, and the gap between the sand samples is larger. As shown in Figure 4d, the sample micrograph with an incorporation ratio of 5% showed that there was more mass cementation on the surface and clearance of standard sand and higher degree of cementation between grains.

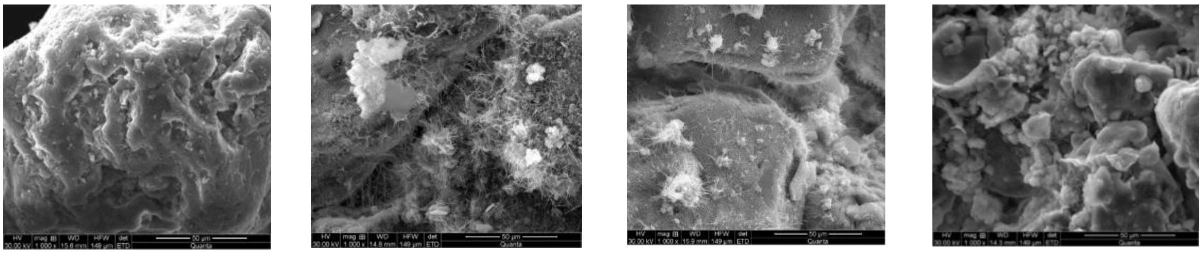

(a) SEM image of quartz sand (magnification 1000 times)

(b) C_v = 2% sample SEM image (magnification 1000 times)

(c) C_v = 3% sample SEM image (magnification 1000 times)

(d) C_v = 5% sample SEM image (magnification 1000 times)

Figure 4. SEM photos of cement sample in 7 days.

As shown in Figures 3 and 4, from the analysis of the cementation mechanism of artificially cemented sand, the main reason for this phenomenon (The strength of the sample increases with the incorporation ratio of cement clinker) is that the cement clinker reacts with water to form hydrated calcium silicate and free calcium hydroxide, the free calcium hydroxide reacts with CO_2 in the surrounding environment to form a $CaCO_3$ precipitate. A part of hydrated calcium silicate and $CaCO_3$ precipitate attaches to the surface of quartz sand and a part fills the gap between quartz sand. Due to the large initial porosity of the selected standard sand, the incorporation of low content (2%) of cement clinker can not completely achieve the higher density of the sample in the same curing time. Therefore, with the increase of the cement clinker mixing ratio, the compactness of the sample is strengthened, and the strength of the sample is continuously improved; on the other hand, the products after hydration of the cement (calcium silicate hydrate and calcium carbonate, etc.) increase. The hydrated calcium silicate and calcium carbonate have a certain strength, which also enhances the strength of the sample.

3.2. The Relationship between Unconfined Compressive Strength and Cement Incorporation Ratio

It can be seen from Figure 4 that the strength of the sample increases as the cement clinker content increases. Figure 4 is a test result of unconfined compressive strength of cemented sand with dry density of 1.65g/cm^3, moisture content of 10%, cement clinker content of 2%, 3% and 5% respectively.

By analyzing the indoor experiment of artificially cemented sand, the unconfined compressive strength of artificially cemented sand is linearly related to the incorporation ratio of 1/ C_v, and the correlation coefficient R^2 of the corresponding linear equation is all greater than 0.97. Therefore, the incorporation ratio has a good correlation with the unconfined compressive strength, and the fitting curve satisfies the test requirements.

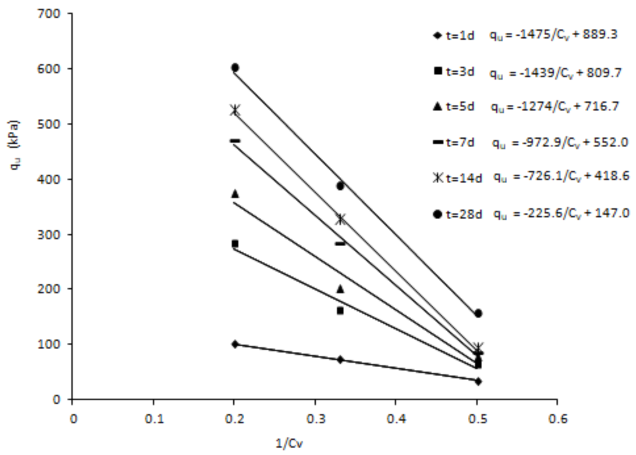

Figure 5. Relationships between unconfined compressive strength (q_u) and clinker cement ratio (C_v) of artificially cemented sand.

Figure 5 shows that the unconfined compressive strength q_u of the artificially cemented sand and the incorporation ratio C_v satisfy the linear equation:

$$q_u = -K\left(\frac{1}{C_v} - \frac{1}{R}\right) \tag{1}$$

In the formula, K is the negative of the slope of the line, which can be considered as a scalar quantity over time. As the curing time increases, the unconfined compressive strength intersects the linear equation of the cement clinker incorporation ratio. And (1) shows that for a mixed soil sample with a certain incorporation ratio, R can be regarded as a constant, that is, the R value obtained by the intersection of each straight line equation at a point. R = 1.77 was obtained by linear regression analysis.

It can be seen from Figure 5 that there is a relationship between the variable K and the curing time t. Through the regression curve analysis (Figure 6), the logarithm of the variable K and the curing time t is obtained. The fitting equation is as follows:

$$K=399.4\ln(t)+311.4 \tag{2}$$

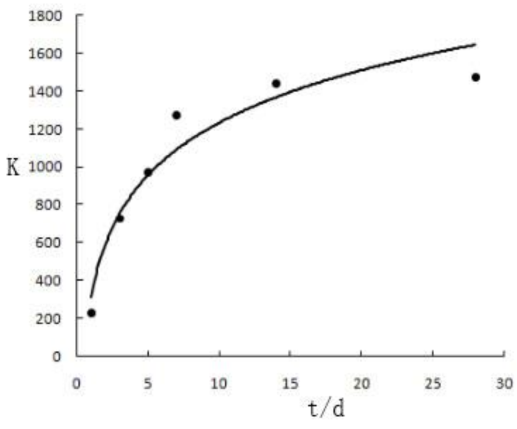

Figure 6. Relationships between K and curing time (t).

It can be seen from equation (1) and (2) that there is a unique functional correspondence between K as a variable, incorporation ratio C_v, and curing time. Therefore, the equation of the relationship between unconfined compressive strength q_u, incorporation ratio C_v and curing time t can be obtained:

$$q_u = (399.4\ln(t) + 311.4)(\frac{1}{R} - \frac{1}{C_v}) \tag{3}$$

3.3. The Relationship Between Unconfined Compressive Strength and Curing Time

The relationship between curing time t and unconfined compressive strength q_u of artificially cemented sand is shown in Figure 7. As the curing time increases, the unconfined compressive strength of the sample gradually increases.

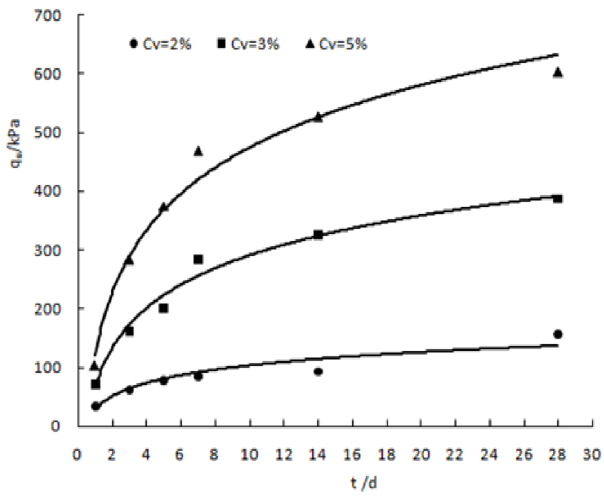

Figure 7. Relationships between unconfined compressive strength (q_u) and curing time (t) of artificially cemented sand.

The equations with different incorporation ratios were obtained by fitting the curves of the unconfined intensity and the curing time.

When the ratio of incorporation is C_v = 2%, the curve equation is:

$$q_u = 33.09\ln(t)+26.8 \tag{4}$$

When the ratio of incorporation is C_v = 3%, the curve equation is:

$$q_u = 97.97\ln(t)+65.25 \tag{5}$$

When the ratio of incorporation is C_v = 5%, the curve equation is:

$$q_u = 153.2\ln(t)+121.5 \tag{6}$$

Since the relationship between the previously fitted unconfined compressive strength q_u and the incorporation ratio C_v and the curing time t satisfies the formula (3), it can be concluded that there is a logarithmic relationship between unconfined strength and curing time under the same incorporation ratio. This is different from the curve equation of the unconfined strength q_u and the curing time t measured by the experiment, but by comparing the measured value with the predicted value, it is found that the prediction equation curve and the experimentally obtained equation curve are both good fits to the unconfined strength and the curing time. It can be seen from Table 4 that the relative error between the measured value and the predicted value is less than 15%, so the unconfined compressive strength prediction equation (3) is established. This has certain guiding significance for the prediction of the strength of weakly cemented sand in engineering.

Table 5. Comparison of measured and predicted strength of artificial cemented sand.

Incorporation ratio (C_v/%)	Curing time (t/d)	Measured value (kPa)	Predicted value (kPa)	Relative error (/%)
2	1	23.50	20.23	13.91
	3	52.93	48.74	7.92
	5	68.83	61.99	9.94
	7	74.90	70.73	5.57
	14	93.55	88.71	5.17
	28	107.75	106.25	1.39
3	1	71.98	72.13	0.21
	3	162.03	173.74	7.23
	5	200.44	220.99	10.25
	7	283.84	252.12	11.17
	14	326.50	316.24	3.14
	28	387.73	380.35	1.90
5	1	102.27	113.66	11.14
	3	283.05	273.82	3.26
	5	374.80	348.28	7.08
	7	438.90	397.33	9.47
	14	526.53	498.38	5.35
	28	602.45	599.43	5.01

3.4 Verification of the Formula

In order to verify the rationality of the unconfined compressive strength prediction of artificial cementation sand carried out by (3), this paper selects the data related to Px solidified sand in Li Chi (Li Chi 2009) and other papers (take the average of two water content strengths). As shown in Table 5, by comparing the prediction equation with the actual data of the project, it can be seen that when the curing agent is incorporated relatively small (less than 20%), the data deviation except for incorporation ratio of 5% is somewhat large, the prediction of other cement sand strength is More accurate, and the relative error between the two is within the allowable range of the test. It can be seen from the comparison of the strength of the cementing sand with the curing agent incorporation ratio of 8% as shown in Figure 8. The measured value and the predicted value curve of the cemented sand alternately rise with the increase of the curing time, and the difference between the two is small. The measured value curve is close to the linear function, and the predicted value curve is close to the logarithmic function, which is consistent with the formula we predicted earlier. However, other researchers (Zhou Hailong et al. 2014; Cao Zhiguo et al. 2015; Zhang Shiyou et al. 2015) have certain limitations on the strength prediction formula of cement soil, and the relevant tests conducted under specific circumstances are suitable for the corresponding projects. Therefore, the artificial cementation sand prediction equation of this paper has certain practicability for some weak cemented sand (incorporation ratio less than 20%) projects, which provides a certain theoretical basis for sand foundation construction.

Table 6. Comparison between the tested strength and predicted strength.

Incorporation ratio (C_v/%)	Curing time (t/d)	Measured value (kPa)	Predicted value (kPa)
2	7	82	70.75
	14	109.5	88.75
	21	122.5	99.28
	28	161	107.75
5	7	185.5	397.33
	14	271	498.38
	21	422.5	557.49
	28	560.5	599.43
8	7	421	478.98
	14	554	600.79
	21	674.5	672.04
	28	761	722.60
12	7	612	616.14
	14	760	772.84
	21	1037	864.49
	28	1155	929.53

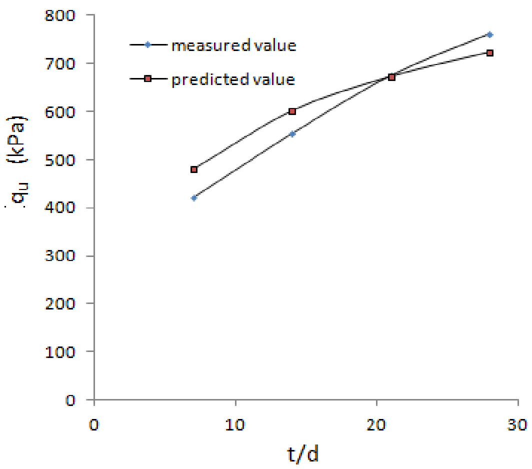

Figure 8. Comparison of measured value and predicted value of unconfined compressive strength of cemented sand with ratio of 8%.

4. Conclusion

(1) The artificially cemented sand has a brittle failure mode in the unconfined compression test.

(2) The micro-morphology of artificially cemented sand with different incorporation ratio ratios at the same curing time was different. The standard sand was magnified 1000 times in the scanning electron microscopy test to be granular and attached with small particles. With the increase of the cement clinker incorporation ratio in the sand sample, the difference of the microscopic morphology of the sand sample is more obvious. The gap between the standard sands is gradually filled by the cement hydration product, and the shape of the cement attached to the surface of the standard sand changes from a filamentous shape to a granular shape.

(3) By analyzing the unconfined compressive strength data of the artificially cemented sand obtained by the test and introducing the variable K value, the fitting formula of the unconfined compressive strength of the artificially cemented sand is proposed. According to the different cement

clinker incorporation ratio and curing time in the formula, the cement sand strength is predicted to be more accurate, and the number of test samples is greatly reduced.

(4) The rationality of the prediction equation is verified by other scholars' research data on the cemented sand, which indicates that the equation has a certain research basis for the low-incorporation ratio of cemented sand, and provides a basis for the construction of the sand foundation.

Acknowledgement
Research Fund of Hubei University of Technology (NO. BSQD14040).

References

[1] Clough G W, et al. (1987). Cemented Sands under Static Loading. Journal of Geotechnical Engineering, 107(GT6): 799-817.
[2] Cao Zhiguo and Zhang Dingwen (2015). Key Parameters Controlling Unconfined Compressive Strength of Soil-Cement Mixtures. Chinese Journal of Rock Mechanics and Engineering, 2015, (S1):3446-3454.
[3] Li Jianhong (2008). A Constitutive Model of Bonded Soil Based on the Micro-Mechanism of Bonding-Breakage. Tsinghua University.
[4] LI Chi and YU Hao (2009). Experimental Studies of Strength Characteristics and Solidified Mechanism for Solidified Aeolian Sandy Soil. Rock and Soil Mechanics, 30 (s2):48-53.
[5] Mitchell J and Soga K (2005). Fundamentals of Soil Behaviour [C], 2005.
[6] Maccarini M (1987). Laboratory Studies of Weakly Bounded Artificial Soil. University of London: London.
[7] Ruan Jinlou, et al (2009). Experimental Study on Cement-soil Unconfined Compressive Strength of Silty Clay. Journal of Railway Science and Engineering, 6 (3):56-60.
[8] Saxena S K and Lastrico M (1987). Static Properties of Lightly Cemented Sand. Journal of Geotechnical Engineering, 104 (GT12): 1449-1464.
[9] Wei Rulong (1986). Technology and Improvement of Soft Clay Soil Picking. Journal of Geotechnical Engineering, 8 (6): 113-125.
[10] Zhang Tianhong, et al. (2013). Intensity of Cement Soil and Influencing Factors. China Railway Science, 24 (6):53-56
[11] Zhao Can (2013). Experimental Research on Mechanics and Constitutive Model of Artificially Cemented Sand. Hubei University of Technology.
[12] Zhou Hailong, et al. (2014). Experiment Research on Unconfined Compressive Strength of Cement Soil Under Small Age [J]. Journal of Shandong University (Engineering Science), 44 (1):75-79.
[13] Zhang Shiyou, et al. (2015). Prediction of Unconfined Compressive Strength of Cement Soil with Different Cement Mixing Amount. Yangtze River, 5 (11):68-70.